Discretization in time gives rise to noise-induced improvement of the signal-to-noise ratio in static nonlinearities

A. Davidović,* E. H. Huntington,† and M. R. Frater‡
School of Information Technology and Electrical Engineering, University College, The University of New South Wales, Canberra, ACT, 2600, Australia

(Received 19 September 2008; revised manuscript received 16 March 2009; published 14 July 2009)

For some nonlinear systems the performance can improve with an increasing noise level. Such noise-induced improvement in static nonlinearities is of great interest for practical applications since many systems can be modeled in that way (e.g., sensors, quantizers, limiters, etc.). We present experimental evidence that noise-induced performance improvement occurs in those systems as a consequence of discretization in time with the achievable signal-to-noise ratio (SNR) gain increasing with decreasing ratio of input noise bandwidth and total measurement bandwidth. By modifying the input noise bandwidth, noise-induced improvement with SNR gain larger than unity is demonstrated in a system where it was not previously thought possible. Our experimental results bring closer two different theoretical models for the same class of nonlinearities and shed light on the behavior of static nonlinear discrete-time systems.

DOI: 10.1103/PhysRevE.80.011119 PACS number(s): 05.40.Ca, 07.50.Qx

I. INTRODUCTION

Noise is generally considered to be an undesirable phenomenon, and considerable effort is expended to reduce or eliminate it. These efforts generally employ filtering, which is essentially a linear process. Unfortunately, filtering can only eliminate the noise that is outside of the band occupied by the signal, i.e., outside of the band of interest. For the noise inside the band of interest, any linear processing will affect the signal and the noise in the same way, and no improvement is possible.

However, under certain conditions, improvements for noisy signals are possible if nonlinear systems are used for processing. Static nonlinearities are of particular theoretical and practical interest since many practical systems can be modeled after them (for example, sensors, quantizers, or limiters). Consequently any performance improvement that they offer will have an impact on a broad range of applications.

In order to characterize the performance improvement various parameters can be used, but in the context of communications and signal processing, the most common one is signal-to-noise ratio (SNR). Others include the Fisher information, entropy, probability of error, etc. SNR gain defined as the ratio of the output to input SNRs is also common. (See for instance [1,2], also [3–6].)

A general theoretical framework enabling analysis of such phenomena in static nonlinearities was published in [7]. In order to facilitate calculations, it employed discretization in time. Some results based on this framework show that in certain cases improvements are possible [7–11]. In addition to that, a possibility of noise-induced improvement of SNR or SNR gain was registered for a number of cases [7,8,11–13]. The SNR or SNR gain showed a peak for a nonzero input noise level. This framework will be referred to as the "discrete-time theory" in the rest of the paper.

By contrast, a much older theory analyzing SNR improvements for bandpass signals processed by static nonlinearities was presented in [14]. It was based on Refs. [15,16] and developed using Fourier-transform methods for continuous-time signals (hereafter referred to as the "continuous-time theory"). The continuous-time theory predicts maximum SNR gains of up to 3 dB for the analyzed nonlinearities, decreasing with the noise level. Theoretical results related to this theory were published in [17,18]. Experiments based on the continuous-time theory have been used for decades, particularly in the field of radio astronomy [19].

On the account of the registered nonmonotonic evolutions of SNR and SNR gain, the authors of [7] claimed a specific type of stochastic resonance.

By contrast, other authors [20,21] argue that stochastic resonance is not possible in static nonlinearities because there are no apparent inherent time scales in such systems.

Both mentioned theories claim to be exact and general, as they are indeed developed with mathematical rigor, but they predict that the same system will exhibit significantly different properties. In this paper we demonstrate that the experimental results for the same type of static nonlinearity, in this case a threshold nonlinearity, will be consistent with predictions of the theory that uses the same approach in its mathematical development. In other words, the physical implementation of the nonlinearity (continuous or discrete time) determines its behavior. An obvious dependence on the sampling frequency in the discrete-time implementation is demonstrated. Our results indicate that discretization in time and aliasing play a key role in obtaining the noise-induced performance improvement, with the SNR gain being dependent on the ratio of input noise bandwidth to total measurement bandwidth.

II. THEORETICAL BACKGROUND

We present a summary of the theoretical results of continuous-time and discrete-time frameworks.

*a.davidovic@adfa.edu.au
†e.huntington@adfa.edu.au
‡m.frater@adfa.edu.au

A. Continuous-time theory

The theoretical framework of the continuous-time theory was developed in [14] for a sinusoidal signal $x(t)=A\sin\omega_s t$ corrupted by narrow-band Gaussian noise being processed by a symmetric nonlinearity. The nonlinearity's transfer characteristic g is assumed to be a nondecreasing odd function of the input, that is, $\{y(t)=g[x(t)]\}$, with x and y being the input and output, respectively. The frequency band of interest is defined by the region in which the input noise spectrum is nonzero. This framework focuses only on that frequency band and assumes that the nonlinearity is followed by a filter that eliminates all harmonics. The following are the equations from [14] that enable the calculation of SNRs and SNR gain.

The powers at the output of the nonlinearity can be calculated from the output autocorrelation function $R_y(\tau)$ at $\tau=0$. The autocorrelation function for the given conditions is

$$R_y(\tau)=2\sum_{\substack{m=1\\(m\ odd)}}^{\infty}h_{m0}^2\cos m\omega_s\tau+\sum_{\substack{k=1\\(k\ odd)}}^{\infty}\frac{h_{0k}^2}{k!}R_N^k(\tau)+2\sum_{\substack{m=1\\(m+k\ odd)}}^{\infty}\sum_{k=1}^{\infty}\frac{h_{mk}^2}{k!}R_N^k(\tau)\cos m\omega_s\tau, \tag{1}$$

where $R_N(\tau)$ is the input noise autocorrelation function, ω_s is the input signal's angular frequency, and coefficients h_{mk} are calculated as

$$h_{mk}(t)=\begin{cases}0, & m+k\ \text{even}\\ \frac{2}{2\pi j}\int_{C^+}f_+(z)e^{\sigma_N^2z^2/2}z^kI_m(zA)dz, & m+k\ \text{odd}.\end{cases} \tag{2}$$

Here, C^+ is a contour along the imaginary axis in the complex plane with a possible indentation to the right of the origin (to avoid singular and branch points). f_+ is the unilateral Laplace transform of the transfer characteristic g on the interval $[0,+\infty)$. σ_N^2 is the power of the input noise, completely contained in the narrow band around the signal frequency. I_m is the mth-order modified Bessel function of the first kind, and A is the input signal amplitude.

Equation (1) contains terms for all signal and noise components at all frequencies. It is arranged so that the first sum contains the output signal terms due to the interaction of the input signal with itself, and the remaining two sums contain terms resulting from the input noise interacting with itself and with the input signal. Since the focus is on the band around ω_s, only those terms that contribute to that frequency band are of interest. After selecting the relevant terms, multiplying them with factors that represent the fractions of those terms that appear in the band of interest (the detailed process is described in [14]), and setting $\tau=0$, the powers at the output can be calculated.

From the signal part of Eq. (1), the output signal power at frequency ω_s can be calculated as

$$P_{S_o}=R_{S_o}(0)=2h_{10}^2, \tag{3}$$

where $R_{S_o}(\tau)$ is the autocorrelation of the output signal (it only contains the term for $m=1$ from the first sum) and coefficient h_{10} is calculated as described above. All other terms contributing to the first sum are eliminated by the filter.

The output noise power in the narrow band of interest around ω_s can be broken down into (i) the component due to the noise interaction with itself $P_{N_o(N\times N)}$ and (ii) the component of the output noise power which is due to the noise interaction with the signal $P_{N_o(S\times N)}$.

These components can be calculated as

$$P_{N_o(S\times N)}=1\times\frac{h_{01}^2}{1!}R_N(0)+\frac{3}{4}\times\frac{h_{03}^2}{3!}R_N(0)^3+\frac{5}{8}\times\frac{h_{05}^2}{5!}R_N(0)^5+\frac{35}{64}\times\frac{h_{07}^2}{7!}R_N(0)^7+\cdots \tag{4}$$

and

$$P_{N_o(N\times N)}=\frac{1}{2}\times2\times\frac{h_{21}^2}{1!}R_N(0)+\left(\frac{3}{4}\times2\times\frac{h_{13}^2}{2!}+\frac{1}{4}\times2\times\frac{h_{32}^2}{2!}\right)R_N(0)^2+\left(\frac{1}{2}\times2\times\frac{h_{23}^2}{3!}+\frac{1}{8}\times2\times\frac{h_{43}^2}{3!}\right)R_N(0)^3+\left(\frac{5}{8}\times2\times\frac{h_{14}^2}{4!}+\frac{5}{16}\times2\times\frac{h_{34}^2}{4!}+\frac{1}{16}\times2\times\frac{h_{54}^2}{4!}\right)R_N(0)^4+\cdots, \tag{5}$$

where $R_N(0)$ is the input noise power (equal to σ_N^2) and the h_{mk} coefficients are calculated as described in Eq. (2).

As the total noise output power is $P_{N_o}=P_{N_o(S\times N)}+P_{N_o(N\times N)}$, the SNR gain is calculated as

$$G_{\mathrm{SNR}}=\frac{P_{S_o}}{P_{N_o}}\frac{\sigma_N^2}{A^2/2}. \tag{6}$$

In [14], exact expressions were obtained via confluent hypergeometric functions for "rooter" nonlinearities of the type $y=x^{1/\nu}$. Asymptotic behavior for $\sigma_N\to0$ and $\sigma_N\to\infty$ was calculated for a hard threshold nonlinearity ($\nu\to\infty$) and can serve as a check for numerical models.

B. Discrete-time theory

Discrete-time theory was developed in [7] for an arbitrary periodic signal corrupted by ideally white noise processed by an arbitrary static memoryless nonlinearity. The conditions for the input signal, noise statistics, and the type of nonlin-

earity are more relaxed than in [14], but a strong requirement of noise whiteness is assumed in order to obtain explicit results.

White noise, however, is a purely mathematical idealization with infinite power ($\sigma_N \to \infty$) and a Dirac δ function as autocorrelation. Physically, it is unrealizable as all physical noises have a finite bandwidth. To facilitate calculations and keep the results exact, the authors move to the discrete-time domain. It is assumed that all quantities are periodically sampled with a sampling interval Δt that is much smaller than the signal period. The move to the discrete-time domain also resolves the issue of noise whiteness. Namely, the noise bandwidth is inversely proportional to its correlation time τ_c and by choosing $\Delta t > \tau_c$, the resulting discretized noise is "whitened." From the general expression given in [7], the SNR ($\mathcal{R}$) of the output at the input signal frequency can be calculated as

$$\mathcal{R}_{out} = \frac{|\overline{Y_1}|^2}{\langle \mathrm{var}[y(t)] \rangle \Delta t \Delta B}. \tag{7}$$

The signal component at the output is the cyclostationary expectation of the total output $E[y(t)]$. Its power is the squared absolute value of the Fourier coefficient at the fundamental frequency, which is in turn calculated as

$$\overline{Y_1} = \langle E[y(t)] e^{-j(2\pi/T)t} \rangle, \tag{8}$$

where $\langle \ldots \rangle$ denotes stationarization by time averaging over one signal period, T, which is performed in N discrete-time points determined by the sampling interval. The discretization interval in the denominator is a result of the Fourier transformation of the normalized stationary autocovariance of the output. This autocovariance is generally difficult or impossible to obtain but, for discrete white noise it evaluates to a constant Δt. $\langle \mathrm{var}[y(t)] \rangle$ is the stationarized variance of the output signal. The product of these two terms determines the output noise power spectral density. To obtain the noise power in the narrow band around the signal, it is multiplied by that bandwidth ΔB.

$\langle \mathrm{var}[y(t)] \rangle$ is calculated from the nonstationary expectations $E[y(t)]$ and $E[y(t)^2]$:

$$E[y(t)] = \int_{-\infty}^{+\infty} g(\xi) f_n[\xi - x(t)] d\xi, \tag{9}$$

$$E[y(t)^2] = \int_{-\infty}^{+\infty} g(\xi)^2 f_n[\xi - x(t)] d\xi. \tag{10}$$

The input SNR for the discretized signal plus noise mixture is

$$\mathcal{R}_{in} = \frac{A^2}{4\sigma_N^2 \Delta t \Delta B}, \tag{11}$$

where A is the input signal amplitude, σ_N^2 is the total input noise power, and Δt comes from the result for the power spectral density of the white discrete input noise.

Hence

$$G_{\mathrm{SNR}} = \frac{|\langle E[y(t)] e^{-j(2\pi/T)t} \rangle|^2}{\langle \mathrm{var}[y(t)] \rangle} \frac{4\sigma_N^2}{A^2}. \tag{12}$$

The discrete-time framework is more general than the continuous-time one and can be used to analyze all the nonlinearities and inputs for which the continuous-time framework was developed but with one major difference—the input noise must be white as opposed to strictly narrowband. This difference is the reason why total noise powers are used in continuous-time framework formulas, and the discrete-time framework works with noise power spectral densities. It must be taken into consideration when comparing the results obtained from the two for the same nonlinearity. Although the results from both frameworks are usually plotted against the input noise rms amplitude σ_N, in the continuous-time framework σ_N is rms amplitude of narrowband noise, while in the discrete-time framework it refers to rms amplitude of discrete white noise. Equations (6) and (12) have a similar shape, but their first terms, representing the output SNR, are rather different in the way they are calculated. The former is obtained by integrating continuous functions, and the latter is obtained by averaging in the discrete-time domain, with assumed undersampling. Having in mind that second terms in both equations are constant, any differences between them should stem from different approaches in calculating the output SNR.

C. Predicted behavior

SNR gain was analyzed as a function of input noise level for a threshold nonlinearity with threshold voltage $V_{th} = 0$ V by using both continuous-time and discrete-time frameworks. Its functional description is given in Eq. (13);

$$V_{out} = \begin{cases} 1 & \text{for } V_{in} > V_{th} \\ 0 & \text{for } V_{in} = V_{th} \\ -1 & \text{for } V_{in} < V_{th.} \end{cases} \tag{13}$$

The input signal was a sinusoid corrupted by the Gaussian noise. As stated previously, for the former the input noise was narrowband and for the latter it was assumed to be ideally white. On the functional level, this is the only difference between them, but it has to be kept in mind, since it means that they are plotted against different x axes. Particularly, in practical experimental measurements, if they are to be plotted against the same abscissa, one of them needs to be scaled appropriately. Figure 1 shows predictions of SNR gain for both cases (plotted on the same graph, for convenience, but bearing in mind the different nature of σ_N). They are strikingly different, both in values and trends, especially in the low noise region. The continuous-time theory predicts SNR gain of approximately 3 dB as $\sigma_N \to 0$, which then decreases monotonically as the noise level increases, and eventually asymptotes to −0.77 dB. On the other hand, the discrete-time theory predicts a nonmonotonic evolution of SNR gain,

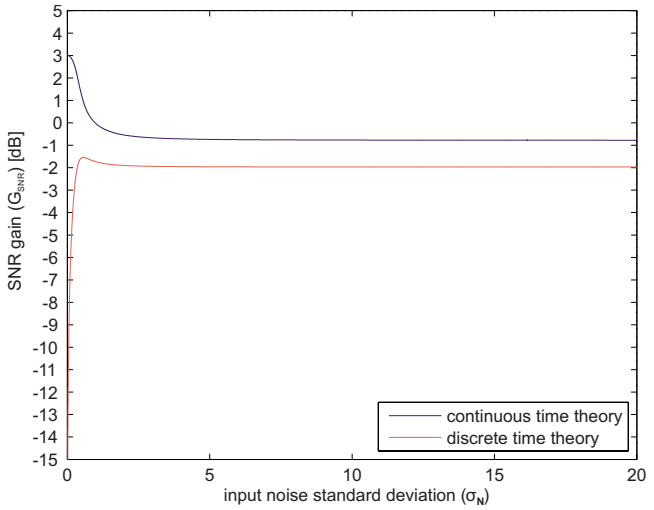

FIG. 1. (Color online) Predictions of the continuous-time and discrete-time theories.

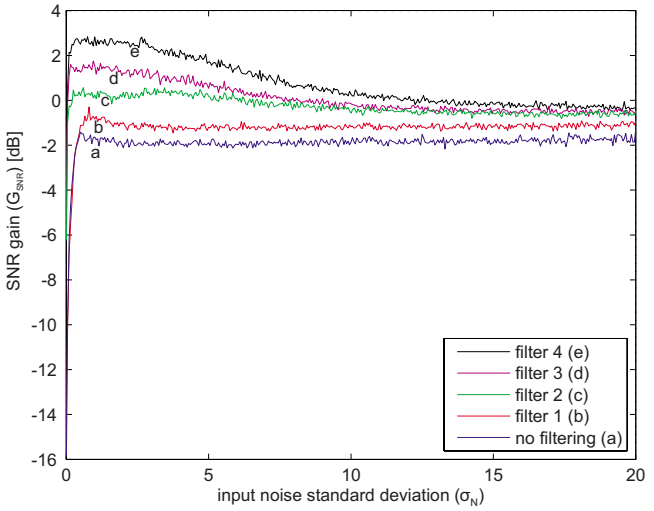

FIG. 2. (Color online) Simulation results for signal-to-noise ratio gains for white input noise and four cases of bandpass noise. The bottom curve is obtained in the case without filtering. The curve above it is for 10 kHz bandwidth ("filter 1") and the filter bandwidths are then getting progressively narrower going upwards ("filter 2"—260 Hz, "filter 3"—200 Hz and "filter 4"—160 Hz, respectively). The fourth case corresponds to the narrowband input as required by the continuous-time theory. σ_N values at filter input are normalized to signal amplitude.

which falls sharply as $\sigma_N \to 0$, has a peak at approximately $\sigma_N = 0.56$ and converges to −2 dB as the noise increases. This theory predicts no SNR gain at all—the output SNR is consistently below that at the input.

The two theories give two clearly different predictions for the same nonlinearity, with the only difference between the systems analyzed is the bandwidth of the input noise, and the assumption of discrete or continuous time.

D. Simulations with finite bandwidth

The discrete-time theory provides exact results for white noise and approximates results for some special cases of correlated noise. So far it has not been successfully extended to cover bandpass noises. With narrowband nature of the input noise being an essential requirement for the applicability of the continuous-time theory, linking the two analytically in an exact manner is not yet possible. Instead, a series of numerical simulations was run in MATLAB, with varying noise bandwidths—starting with an infinite bandwidth white Gaussian noise (as in the discrete-time theory) and finishing with a narrowband one (simulating the discrete-time experiment that follows).

Simulations' parameters are given in Table I. The sampling rate and signal frequency were chosen to reflect the relationships in the experiment that follows.

TABLE I. Simulations' parameters.

Sampling frequency (F_s)	44100 Hz
Signal frequency (f)	89 Hz
Signal amplitude (A)	1
Noise rms amplitude (σ_N)	Variable (from 0.01 to 20)
Filter	Butterworth type bandpass with changing bandwidths
Window type and length	Hann, 44100 samples
Number of FFT points	2^{16}

The SNR is defined in terms of the ratio of power spectral densities integrated over a known bandwidth. For continuous time,

$$\mathcal{R} = \int_{\Delta \mathbb{B}_S} S(\omega) d\omega \Big/ \int_{\Delta \mathbb{B}_N} S(\omega) d\omega. \tag{14}$$

In discrete time, SNR can be calculated as (see [22,23])

$$\mathcal{R} = \sum_{k \in \Delta B_S} S_{DFT}(k) \Big/ \sum_{k \in \Delta B_N} S_{DFT}(k), \tag{15}$$

where $\mathcal{R}$ is the SNR and S is the power spectral density of the noisy signal, S_{DFT} is its discrete estimate obtained using discrete Fourier transform (using the Welch's periodogram method [24]). The spectral resolution of the measurement is determined by the integration time of the measurement. $\Delta \mathbb{B}_S$ (ΔB_S) is the narrow continuous (discrete) frequency band around the signal frequency (index closest to the signal frequency) and $\Delta \mathbb{B}_N$ (ΔB_N) is the band of noise measurement around or near the signal frequency (index closest to the signal frequency).

The simulations' results are shown in Fig. 2. It is obvious that the simulation for ideally white noise corresponds to the prediction of the discrete-time theory. Reducing the noise bandwidth (compared to the total measurement bandwidth) results in increasing the SNR gain, while the general shape of the curves is preserved. Finally for the narrowband case (as required in Sec. II A), the maximum gain corresponds to the predictions of the continuous-time theory, as does the asymptotic value as $\sigma_N \to \infty$. However, there is an important difference. The simulation shows a noise-induced improvement of SNR gain for the narrowband case, which is in con-

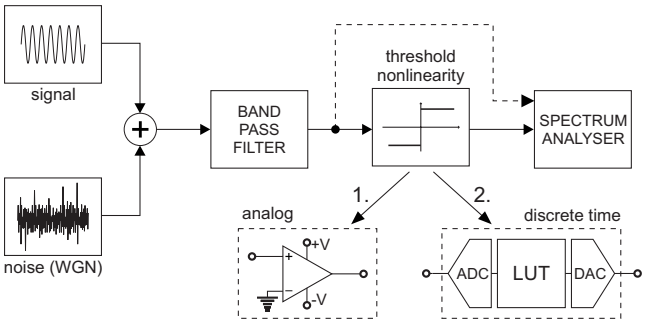

FIG. 3. Experimental setup with continuous (1.) and discrete time (2.) nonlinearity. WGN stands for "white Gaussian noise."

flict with predictions of the continuous-time theory. This is interesting since the only difference between them is discretization in time, and the Nyquist criterion is satisfied.

III. EXPERIMENTAL RESULTS AND DISCUSSION

In order to investigate the effects that discretization in time has on static nonlinearities and how the parameters of discretization affect their behavior, two experiments were conducted. The first experiment shows that the behavior of the nonlinearity can agree with predictions of both theories, depending on its physical implementation. The second experiment shows the connection between the inherent time scale of the discretization process and the observed results.

A. Continuous time vs discrete time

In the first experiment, the system from Fig. 3 was implemented. The threshold nonlinearity with threshold voltage $V_{th}=0$ V was first realized as an analog continuous-time circuit and then in a discrete-time implementation. Its functional description is given as

$$V_{out} = \begin{cases} V_{sat} & \text{for } V_{in} > V_{th} \\ 0 & \text{for } V_{in} = V_{th} \\ -V_{sat} & \text{for } V_{in} < V_{th}. \end{cases} \quad (16)$$

In the experimental setup, two Agilent 33220A function generators were used, one as the signal and the other as the noise source. The guaranteed white noise power spectral density for these generators is up to 9 MHz. As the band of interest in the experiment was in a much lower-frequency range and the filter bandwidth was narrow, the noise was locally white. The adder circuit was a standard unity-gain inverting adder, the filter was an active two stage band pass filter, and the analog threshold nonlinearity was an open-loop operational amplifier, which approximates the characteristic given in Eq. (16) very well. All analog circuits were built around high-speed large bandwidth LM6361N operational amplifiers.

For the discrete-time implementation of the nonlinearity a digital signal processing board based around a Xilinx SpartanXL chip was used. The board contains standard analog signal conditioning circuitry, analog-to-digital converter (ADC), and digital-to-analog converter (DAC) and between them a look-up table (LUT) into which the transfer characteristic can be programmed. The sampling rate was 50 MHz, and conversion resolution was 8 bits/sample.

TABLE II. Experiment system parameters.

Signal frequency	100 kHz
Signal amplitude (A)	9, 0.5, and 0.25 V
Normalized noise rms (σ_N)	Variable (from 0.2 to 20)
Filter	Two stage second-order Sallen-Key bandpass with 98 kHz and 102 kHz corner frequencies

The measurements of signal and noise powers were performed on a spectrum analyzer, with resolution and video bandwidths set to 300 Hz and video averaging to 30 passes. The analyzer measures the power spectral density of the input signal, integrated over the passband of the input filters. Thus, it is possible to directly read the power for the set bandwidth at any frequency. (More details on the spectrum analyzer operation can be found in [25].) Other system parameters are given in Table II.

In order to obtain lower values of the normalized σ_N, the signal amplitude from the "signal" function generator was kept constant, and the noise power from the "noise" function generator was increased.

Figures 1 and 2 indicate biggest differences for small values of σ_N. Figure 4 shows the experimental results overlaid with theoretical predictions from Eqs. (6) and (12) and simulation results for no filtering and a narrowband filter (as in the discrete-time theory and in discrete-time experiment), respectively. In order to plot the continuous-time theory curve in the same figure, the scaling factor of 0.022 for its horizontal axis was determined from the measurements of the filter's output noise rms value for different values of input σ_N. The

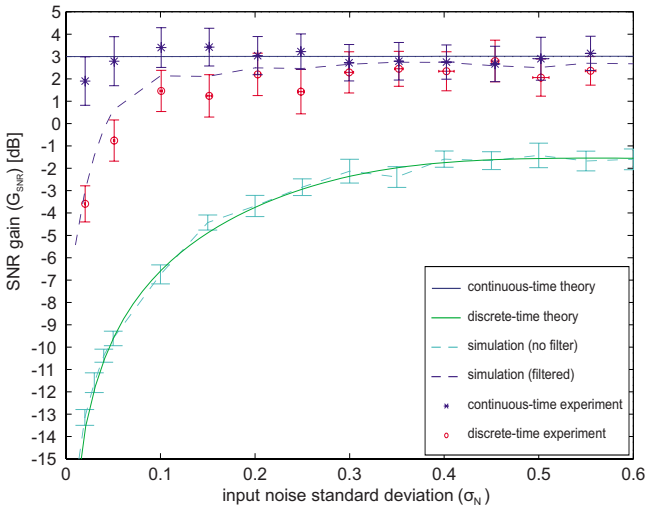

FIG. 4. (Color online) signal-to-noise ratio gains, experimental, simulated, and theoretical. σ_N values at filter input are normalized to signal amplitude. Error bars for simulation with filtering are approximately the same as for the simulation without filtering. The "simulation (filtered)" curve corresponds to the filter 4 curve from Fig. 2.

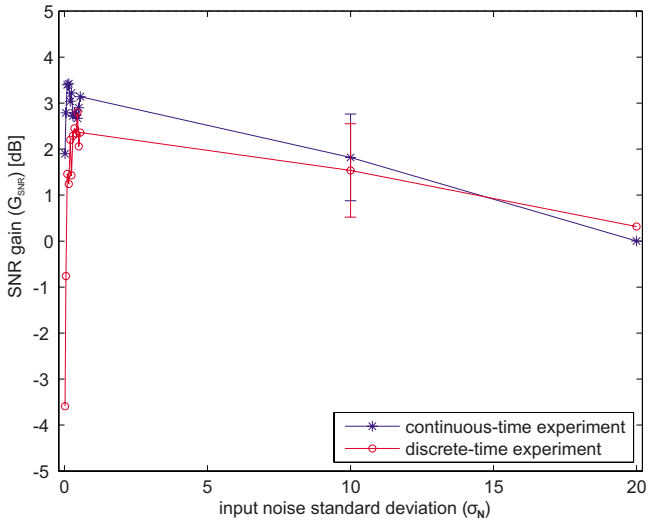

FIG. 5. (Color online) Experimental measurements of signal-to-noise ratio gains, analog, and discrete time. σ_N values at filter input are normalized to signal amplitude. Error bars for all measurements are approximately the same as those shown in the plot.

SNR gain measurements in the continuous-time nonlinearity remain around 3 dB, within the measurement error for low values of the input noise. The behavior in the discrete-time case is significantly different. Here the SNR gain decreases sharply for very low values of σ_N, approaching the values from the continuous-time measurements as the input noise grows. We see a clear case of noise-induced SNR improvement as predicted by the discrete-time theory.

Overall, the analog experimental results agree with the continuous-time theory within error-bars, while the digital experimental results display trends predicted by the discrete-time theory but with different absolute values. The numerical simulations of the discrete-time implementation agree well with the discrete-time experiment for narrow-band noise and the discrete-time theory for white noise.

We notice that noise-induced improvement is registered in the predictions of the discrete-time theory, the digital implementation of the nonlinearity, and in both simulations. What they have in common is the presence of discrete-time signal processing. By contrast, in the continuous-time implementation of the nonlinearity there is no noise-induced improvement nor is it predicted by the continuous-time theory.

To obtain a complete picture, additional measurements were done for two large values of σ_N and the results are shown in Fig. 5. For the normalized values of $\sigma_N=10$ and $\sigma_N=20$ the noise power from noise function generator was kept constant and the signal power from signal function generator was reduced. In both cases, the gain decreases for large levels of input noise. The continuous-time implementation of the nonlinearity displays a monotonic decrease in SNR gain, while the discrete-time implementation displays noise-induced SNR improvement, both in line with predictions of the respective theories.

Nonlinear processing in discrete time inevitably causes aliasing, which does not happen in either analog or linear discrete-time systems. As shown in [17,16], when band limited noise passes through a nonlinearity, its spectral power is spread outside the original band, and its harmonics appear at higher frequencies. In a discrete-time system, any harmonic component above $F_s/2$ will be aliased into the band determined by the sampling rate. We hypothesize that the aliased spectrally correlated components of both signal and noise, and the way they are added up [26,27], may be the cause of the different behavior of systems with discrete-time processing and of the noise-induced SNR improvement they display. This is a matter for further investigation.

It should be noted that aliasing is implied in the discrete-time theory since the condition $\Delta t > \tau_c$ can be interpreted as deliberate aliasing.

B. Influence of the discretization time

The connection between sampling, sampling rate, and SNR in nonlinear processing of discrete-time signals is not unknown. It has been noticed in works related to radio astrophysical spectral measurements [28,29] where sampling and threshold-nonlinearity processing were both done in one step (one-bit sampling). It was shown that, in the conditions of very low input SNR, increasing the sampling rate beyond the Nyquist criterion improves the SNR at the output of correlational receivers.

As mentioned in Sec. I, some authors have argued that nonmonotonic evolution of the performance of static nonlinearities as a function of noise is a signature of stochastic resonance. Others, however argue that this is not the case, since there is no characteristic time scale present in the system itself. In their view, this phenomenon should be considered as a special case of the "dithering" effect. Dithering arises from discretization in amplitude, and it is generally considered that if sampling is "properly applied," it is "error-free" [20]. The generally accepted rule in linear digital signal processing is to satisfy the Nyquist criterion. The effects observed in the experiment described here arise from discretization in time, which cannot be ignored in spite of the sampling rate being well above the Nyquist rate. In fact, the Nyquist criterion cannot be applied blindly even in the case of simple processing as shown in [30]. In order to avoid aliasing, the rate at which the signal is periodically sampled needs be matched to the subsequent signal processing. With nonlinear processing the only way to completely avoid aliasing in this scenario would be to increase the sampling rate to infinity.

Discretization in time has its own "characteristic time scale"—the sampling period. It is therefore interesting to characterize how the relationship between F_s, signal frequency and bandwidth affects the SNR behavior and noise-induced improvements for low-pass signals, which are the most common case in signals discretization.

To investigate this, the system from Fig. 3 was modified as shown in Fig. 6. The nonlinearity was analog, and the signals were acquired at points 1 and 2 using a 10-bit digitizer with a variable sampling frequency. The analysis was done on a PC using MATLAB. System parameters are given in Table III.

Power spectral densities were estimated using periodogram method, with Hann window of variable length, in

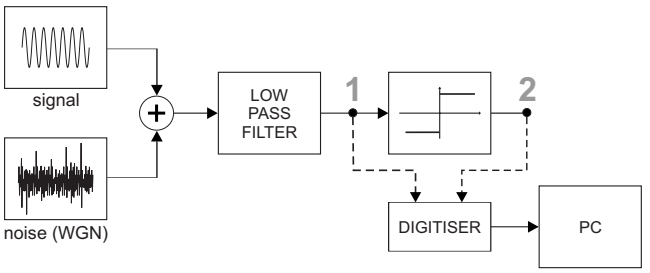

FIG. 6. Experimental setup for the second experiment. WGN stands for white Gaussian noise.

order to keep the frequency resolution for different sampling frequencies constant.

Figure 7 shows that for larger σ_N the SNR gain increases with F_s—behavior similar to that of correlation receivers. When $\sigma_N \to 0$, SNR gain still decreases for all F_s as with the discrete-time nonlinearity and simulations. However, the slope is changed as F_s increases. Larger F_s leads to gains larger than unity but with a less pronounced noise-induced improvement. This is not surprising since the limit case of $F_s \to \infty$ corresponds to continuous time, and the results for an increasing sampling frequency show a tendency toward the continuous-time theory prediction and the continuous-time experiment results from Fig. 4. Changing the relationship among the signal frequency, noise bandwidth, and F_s changes the resonant curves, making this phenomenon frequency dependent.

These results further strengthen the connection between discretization in time and noise-induced improvement of SNR gain. There is indeed a dependence on time scales, that is, on the relationship between the sampling time, signal period, and noise correlation time. This is why such behavior is not observed in the continuous-time system and becomes less pronounced with shorter sampling periods.

IV. CONCLUSION

As we have seen the discrete-time theory predicts noise-induced improvements and nonmonotonic behavior for SNR and SNR gain for static nonlinearities in certain conditions.

On the other hand, the much older continuous-time theory predicts no nonmonotonicity or noise-induced improvements at all for the nonlinearity investigated here.

In our experiment, conducted for a threshold static nonlinearity, we have demonstrated that a system with one functional description can display different behaviors, depending on its implementation details. If the nonlinearity is implemented in continuous time, it behaves as predicted by the continuous-time theory, and if it is implemented in discrete time, it follows the predictions of the discrete-time theory. We have also demonstrated the importance of discretization in time for obtaining the noise-induced improvement of SNR gain.

TABLE III. Second experiment system parameters.

Signal frequency	90 kHz
Sampling frequency	Variable (500 kHz–5 MHz)
Data record length	1048064 samples (for all sampling frequencies)
Normalized noise rms (σ_N)	Variable (from 0.1 to 2)
Filter	Two stage fourth-order Sallen-Key low-pass with 200 kHz corner frequency

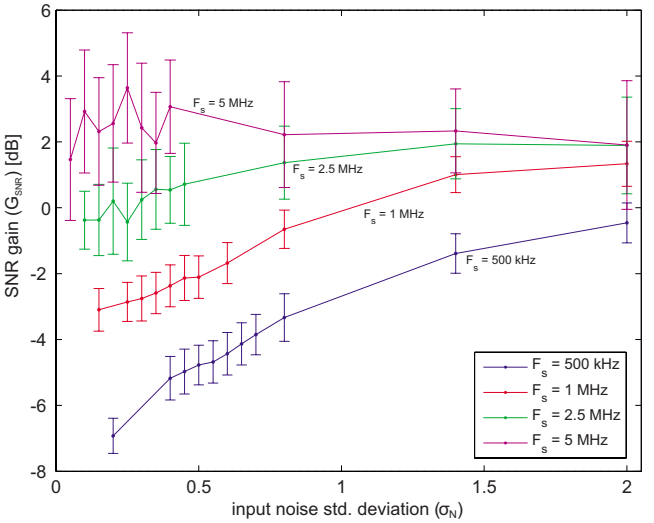

FIG. 7. (Color online) Dependence of signal-to-noise ratio gain curves on the sampling rate F_s, (σ_N values at filter input, normalized to signal amplitude).

The authors of the discrete-time theory argue there that the results obtained there represent a specific type of stochastic resonance found only in static nonlinearities. Their independence on frequency is seen as an advantage over the dynamic stochastic resonant systems.

Other authors, however, argue that the observed effects are not stochastic resonance at all, precisely for the mentioned lack of frequency dependence and characteristic time scale. In their view these effects should be considered a special case of dithering.

The proponents of the "dithering explanation" ignore discretization in time, assuming that it is enough to have a high enough sampling rate. As demonstrated here, the effects of discretization in time cannot be ignored even for high sampling rates. Moreover, discretization in time has a characteristic time scale—the sampling interval, whose influence disappears only in the limit case of the infinite sampling rate.

These results contribute to the ongoing debate on whether or not static nonlinearities display stochastic resonance and what conditions lead to such behavior. Just as importantly, they indicate that the Nyquist criterion cannot be applied blindly in nonlinear digital signal processing. An observation that may profoundly affect the range of applications to which digital signal processing may be applied.

ACKNOWLEDGMENTS

This work was supported by the Australian Research Council.

[1] B. P. Lathi, *Modern Digital and Analog Communication Systems*, 3rd ed. (Oxford University Press, New York, 1998).
[2] H. Van Trees, *Detection, Estimation, and Linear Modulation Theory* (Wiley and Sons, New York, 2001).
[3] J. W. C. Robinson, D. E. Asraf, A. R. Bulsara, and M. E. Inchiosa, Phys. Rev. Lett. **81**, 2850 (1998).
[4] A. Neiman, B. Shulgin, V. Anishchenko, W. Ebeling, L. Schimansky-Geier, and J. Freund, Phys. Rev. Lett. **76**, 4299 (1996).
[5] C. Heneghan, C. C. Chow, J. J. Collins, T. T. Imhoff, S. B. Lowen, and M. C. Teich, Phys. Rev. E **54**, R2228 (1996).
[6] I. Goychuk and P. Hänggi, Phys. Rev. E **61**, 4272 (2000).
[7] F. Chapeau-Blondeau and X. Godivier, Phys. Rev. E **55**, 1478 (1997).
[8] F. Chapeau-Blondeau, Phys. Lett. A **232**, 41 (1997).
[9] F. Chapeau-Blondeau and D. Rousseau, Phys. Rev. E **70**, 060101(R) (2004).
[10] F. Chapeau-Blondeau and D. Rousseau, Electron. Lett. **41**, 618 (2005).
[11] F. Chapeau-Blondeau and D. Rousseau, Circuits Syst. Signal Process. **25**, 431 (2006).
[12] F. Chapeau-Blondeau, Chaos **9**, 267 (1999).
[13] D. Rousseau and F. Chapeau-Blondeau, Phys. Lett. A **321**, 280 (2004).
[14] W. B. Davenport, Jr., J. Appl. Phys. **24**, 720 (1953).
[15] S. O. Rice, Bell Syst. Tech. J. **24**, 46 (1945).
[16] D. Middleton, Q. Appl. Math. **5**, 445 (1948).
[17] J. H. Van Vleck and D. Middleton, Proc. IEEE **54**, 2 (1966).
[18] J. C. Springett and M. K. Simon, IEEE Trans. Commun. Technol. **19**, 42 (1971).
[19] J. B. Hagen and D. T. Farley, Radio Sci. **8**, 775 (1973).
[20] L. Gammaitoni, Phys. Rev. E **52**, 4691 (1995).
[21] L. Gammaitoni, Phys. Lett. A **208**, 315 (1995).
[22] W. D. Gregg, *Analog and Digital Communication* (Wiley and Sons, New York, 1977).
[23] P. Stoica and R. Moses, *Introduction to Spectral Analysis* (Prentice Hall, Englewood Cliffs, NJ, 1997).
[24] P. D. Welch, IEEE Trans. Audio Electroacoust. **15**, 70 (1967).
[25] Agilent Application Note 150, Agilent Spectrum Analysis Basics.
[26] W. A. Gardner, Signal Process. **11**, 13 (1986).
[27] W. A. Gardner, IEEE Trans. Commun. **35**, 529 (1987).
[28] H. Ekre, IEEE Trans. Inf. Theory **9**, 18 (1963).
[29] W. R. Burns and S. Yao, Radio Sci. **4**, 431 (1969).
[30] I. Bilinskis, *Digital Alias-free Signal Processing* (Wiley and Sons, New York, 2007).